

Optimal Operation Point for the Primary Harmonic Content of a Modulated Laser Diode

MEYSAM BAVAFA, HESAM ZANDI, MAYSAMREZA CHAMANZAR, and SINA KHORASANI
School of Electrical Engineering, Sharif University of Technology
P. O. Box 11365-9363, Tehran, Iran

Abstract: An analysis of harmonic contents of the optical output power for a laser diode is performed, and the results are described in details. The influence of external parameters such as modulation current, bias current, and frequency on the absolute value of power for each harmonic are fully described. The analysis is done by direct solution of rate equations of an arbitrary laser diode for carrier and photon densities. It is shown that the optical power has a nonlinear dependence on modulation frequency, and the maximum optical power of each harmonic attained in its resonance frequency. The resonant frequency is shown to be tunable by bias current; thus in the next step we obtain the power for different harmonic contents, allowing better optimization to gain improved results. We calculate the higher relaxation resonant frequencies, and obtain their relation with respect to lower resonant frequencies. We extend our approach and find an optimal operation point in which the optimum characteristics of laser diode can be achieved. The sequence for every arbitrary laser structure is also possible to be developed by the approach presented in this work.

Keywords: Laser Diode, Optical Modulation, Relaxation Resonant Frequency, Rate Equations, Operation Point.

1 Introduction

The rate equations of a semiconductor laser diode [1] present nonlinear distortions to the output optical power versus input current. This fact can be of importance in transmission of data in the form of amplitude modulation, and can limit the available bandwidth for large-signal modulation ratios.

Cartledge and Srinivasan [2] developed a technique for readily extracting values of the rate equation parameters using measurements of the threshold current, the optical power, resonance frequency, and damping factor for a bias current well above the threshold current. Salgado, Ferreira, and O'Reilly [3] employed a nonlinear analysis to the intermodulation distortion of semiconductor lasers, and could show that the intrinsic parameters of the laser diodes could be recovered from experimental measurements of the intermodulation distortion. Sharaiha [4], [5] applied a harmonic balance approach based on a perturbation method to study the nonlinear response of semiconductor optical amplifiers to the third order.

A technique for the extraction of laser rate equation parameters to be used in the simulation of high-speed optical telecommunication systems is presented by André, A. N. Pinto, J. L. Pinto, and da Rocha [6]. They claimed that their simulation using the extracted parameters is valid even for a large current modulation and soliton pulses.

Chen, Ram and Helkey [7] studied the third-order intermodulation nonlinearity, and showed that it would be possible for various nonlinear effects to cancel each

other by choosing appropriate distributed-feedback structure and facet conditions.

Morthier, Schatz, and Kjebon [8] investigated the occurrence of a second resonance frequency in distributed Bragg reflector laser diodes and the high modulation bandwidth resulting from it. They also studied the possibilities of large-signal digital modulation and the influence of different laser parameters theoretically.

Yildirim and Schetzen [9] discussed the effect of feedback on harmonic distortion of a single-mode laser diode. Ghoniemy, MacEachern, and Mahmoud [10] introduced a comprehensive model for semiconductor laser characteristics such as relaxation-oscillation peak frequency, modulation bandwidth, and evaluated their model under different conditions.

We have recently revisited the problem of harmonic contents in the optical frequency response of a laser diode [11], [12], and obtained expressions for the harmonic distortions introduced into the output of a directly current-modulated laser diode. Here we extend the approach, and show that there is a trade-off between distortion and modulation efficiency. The absolute maximum is shown to appear at the first harmonic resonant frequency, due to the Lorentzian characteristic of the output power. The poles of harmonic powers and their dependency to the bias current are completely analyzed. Because of the square root dependence of the resonant frequency to the current, the bias current can be adjusted to obtain the desired relaxation resonance frequency. Furthermore, we calculate, and show there is an optimal operation point to obtain the maximum primary harmonic power.

2 Theory

2.1 Initializing the Laser Diode

For analyzing the harmonic power content we launch the laser diode by a single frequency (ω) current (I) with amplitude (I_1), and biased with a DC current (I_0); the supposed model can explain the harmonic contents generated for a signal packet containing a frequency spectrum. Hence, the current is given by

$$I = I_0 + I_1 e^{j\omega t}. \quad (1)$$

We have two coupled parameters here: the photon density N_p and electron density N_E , which in this analyze have infinite harmonic contents. Defining N_{p_n} and N_{E_n} as the coefficients of the expansion of the photon density, and electron density over frequency, we can write them down as:

$$N_E = \sum_{n=0}^{\infty} N_{E_n} e^{jn\omega t}, \quad (2)$$

$$N_p = \sum_{n=0}^{\infty} N_{p_n} e^{jn\omega t}. \quad (3)$$

We start our approach by substituting (1)-(3) in rate equations [11]. First harmonic of photon density is generated directly by the first harmonic of current applied to laser diode but higher harmonics are found from recursion equations, as given below. In the general case for an arbitrary integer $k > 1$, the k -th harmonic photon density is calculated from all of the lower harmonics of photon and electron densities. We define the parameter M_k in the form of a summation, which relates the k -th harmonic to the lower ones

$$M_k \triangleq \sum_{n=1}^{k-1} N_{E_n} N_{p_{k-n}}, \quad (4)$$

therefore, we can find the k -th harmonic of the photon and electron densities as [11]

$$\begin{cases} N_{E_k} = \frac{-V_g a \left(1 + \frac{1}{jk\omega\tau_p}\right)}{jk\omega + \frac{1}{\tau_e} + V_g a N_{p_0} \left(1 + \frac{1}{jk\omega\tau_p}\right)} \cdot M_k \\ N_{p_k} = \frac{\Gamma V_g a}{jk\omega} (N_{p_0} N_{E_k} + M_k) \end{cases} \quad (5)$$

where τ_e is the carrier lifetime, a is the differential gain, Γ is the cavity confinement factor, V_g is the cavity volume, and τ_p is the photon lifetime.

2.2 Harmonic Power Contents

In this section, we calculate the power content of the harmonics with some relatively straightforward substitutions. To obtain the power contents, we first construct the stored optical energy in the cavity by

multiplying the photon density N_p by the energy per photon $h\nu$ and the cavity volume V_p . Then, we multiply this by the energy loss rate through the mirrors to get the optical power output [11]. The mirror loss is modeled by the mirror loss time τ_m . By performing a summation on k we will have the Total Output Power:

$$P_{out}|_{Total} = \sum_k \frac{h\nu V_p}{\tau_m} N_{p_k}. \quad (6)$$

2.2 Relaxation Resonant Frequency

The frequency ω_R at which the amplitude of the power harmonic content reaches to its maximum is called the Relaxation Resonant Frequency.

We can obtain the primary harmonic power as

$$\frac{P_1(j\omega)}{I_1(j\omega)} = \frac{h\nu V_g a N_{p_0} \eta_i \frac{1}{\tau_m q}}{\frac{V_g a N_{p_0}}{\tau_p} - \omega^2 + j\omega \left(\frac{1}{\tau_e} + V_g a N_{p_0} \right)}. \quad (7)$$

where η_i is the efficiency coefficient and the cavity confinement factor Γ is written as the ratio of V/V_p . It clearly has two poles at

$$\omega = \pm \left[\frac{1}{\tau_p} V_g a N_{p_0} - \frac{1}{4} \left(\frac{1}{\tau_e} + V_g a N_{p_0} \right)^2 \right]^{\frac{1}{2}} + j \frac{1}{2} \left(\frac{1}{\tau_e} + V_g a N_{p_0} \right) \quad (8)$$

which are located in the first and second quadrants of the complex ω plane. We now notice that the denominator of (7) is minimized at the frequency

$$\omega^2 = \omega_R^2 = \frac{V_g a N_{p_0}}{\tau_p}, \quad (9)$$

where ω_R is called the Relaxation Resonant Frequency. Hence, the denominator becomes pure imaginary, and the primary power harmonic content reaches to its resonance mode. We can apply this approach in finding the higher harmonic resonance frequencies as explained below. Following the approach in [11] we find the second harmonic resonant frequency by substituting the second index in the rate equations. If we rewrite the rate equations in the matrix form, we obtain the following:

$$\begin{bmatrix} 2j\omega & -\Gamma V_g a N_{p_0} \\ \frac{1}{\Gamma \tau_p} & 2j\omega + \frac{1}{\tau_e} + V_g a N_{p_0} \end{bmatrix} \begin{bmatrix} N_{p_2} \\ N_{E_2} \end{bmatrix} = \begin{bmatrix} \Gamma V_g N_{E_1} N_{p_1} \\ -V_g a N_{E_1} N_{p_1} \end{bmatrix}. \quad (10)$$

If we want to compute the relaxation resonance frequency we have to find the frequency response of second harmonic power; here we must consider that the poles of $P_2(j\omega)$ are the same poles of N_{p_2} .

We now define A as the matrix of coefficients in the left hand side of (10)

$$A = \begin{bmatrix} 2j\omega & -\Gamma V_g a N_{p_0} \\ \frac{1}{\Gamma \tau_p} & 2j\omega + \frac{1}{\tau_e} + V_g a N_{p_0} \end{bmatrix}. \quad (11)$$

Considering the matrix equation (10), it can be concluded that the poles of the second harmonic power include the poles of N_{E_i}/I_1 and N_{P_i}/I_1 . In fact, the roots of the matrix equation $|A| = 0$ will characterize the rest of the poles:

$$|A| = -4\omega^2 + \omega_{R_1}^2 + j2\omega \left(\frac{1}{\tau_e} + V_g a N_{p_0} \right) = 0. \quad (12)$$

Consequently we have:

$$P_2(j\omega) = \frac{A_1}{\left\{ 1 - \left(\frac{\omega}{\omega_{R_1}} \right)^2 + j \left(\frac{\omega}{\omega_{R_1}} \right) \left[\omega_{R_1} \tau_p + \frac{1}{\tau_e \omega_{R_1}} \right] \right\}^2} \times \frac{A_2}{1 - \left(\frac{2\omega}{\omega_{R_1}} \right)^2 + j \left(\frac{2\omega}{\omega_{R_1}} \right) \left[\omega_{R_1} \tau_p + \frac{1}{\tau_e \omega_{R_1}} \right]}, \quad (13)$$

where

$$A_1 = \frac{h\nu V_g a N_{p_0} \eta_i}{\tau_m q} \frac{1}{\omega_{R_1}^2} \quad (14)$$

$$A_2 = \frac{-2V_g \eta_i}{\omega_{R_1}^2} \frac{1}{qV_p} \cdot \omega \cdot \left[\omega - \frac{j}{2} \left(\frac{1}{\tau_e} + \omega_{R_1}^2 \tau_p (1+a) \right) \right] \cdot I_1^2$$

Therefore, it can be concluded that the second harmonic power $P_2(j\omega)$ has two resonant frequencies; ω_{R_1} and ω_{R_2} .

We call ω_{R_2} as the second resonance relaxation frequency. Furthermore, (13) yields

$$\omega_{R_2} = \frac{1}{2} \omega_{R_1}. \quad (15)$$

As discussed in the next section, our simulations justify the above result.

If we continue this approach for higher harmonics, the rest of poles similar to the poles of (13) appear for the n -th harmonic, in addition to the lower harmonic poles. This happens because of inverting the coefficient matrix

$$A(nj\omega) = \begin{bmatrix} nj\omega & -\Gamma V_g a N_{p_0} \\ \frac{1}{\Gamma \tau_p} & nj\omega + \frac{1}{\tau_p} + V_g a N_{p_0} \end{bmatrix}, \quad (16)$$

which in fact multiplies its determinant

$$|A(nj\omega)| = \omega_{R_1}^2 - (n\omega)^2 + j \left(\omega_{R_1} n\omega \right) \left[\omega_{R_1} \tau_p + \frac{1}{\tau_e \omega_{R_1}} \right], \quad (17)$$

to the previous poles. Therefore the n -th resonance frequency will be given by

$$\omega_{R_n} = \frac{1}{n} \omega_{R_1}. \quad (18)$$

The location of poles in the complex space for the first four harmonic powers of a typical laser diode is shown in Fig. 1. By increasing the bias current, the distance of poles from the origin increases.

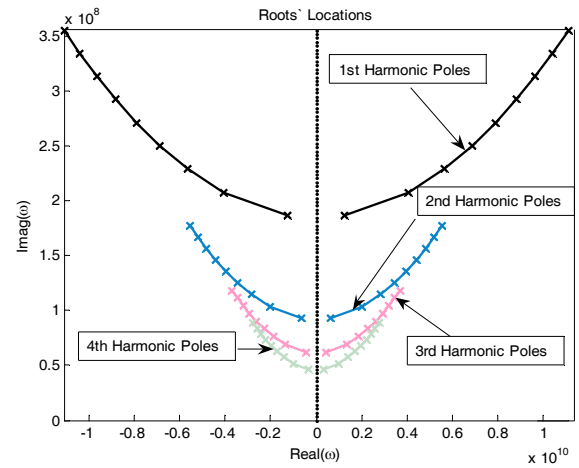


Fig. 1. Location of poles for the first four harmonics power content of laser diode

Due to the dominant pole ω_{R_1} with high recurrence in the denominator of the n -th harmonic power $P_n(j\omega)$ one has

$$P_n(j\omega)|_{\omega=\omega_{R_n}} < P_n(j\omega)|_{\omega=\omega_{R_1}}, \quad (19)$$

which means that each harmonic still has its absolute maximum at the first resonant frequency of the laser diode.

2.3 Optimal Operation Point for Modulation

As discussed earlier the optimum modulation frequency is the resonant frequency which is determined from the bias current. Therefore, the optimal operation point for modulation, where the power of the primary harmonic reaches its maximum, must lie on the curve obtained from the following [1]

$$\omega_{R_1}^2 = \frac{V_g a}{qV_p} \eta_i (I_o - I_{th}). \quad (20)$$

Hence, if we apply (20) into (7), and simplify the result, the peak curve of the first harmonic power will be determined merely by the modulation frequency (resonant frequency):

$$\frac{P_1(j\omega)}{I_1(j\omega)} = -j \frac{h\nu \eta_i}{\tau_m q} \cdot \frac{\omega_{R_1}}{\omega_{R_1}^2 + \frac{1}{\tau_e \tau_p}}. \quad (21)$$

The above equation is not monotonic with respect to frequency, and has a maximum value which is determined by derivation with respect to the modulation frequency. This maximum value occurs in

$$\omega_{R_{Optimum}} = \frac{1}{\sqrt{\tau_e \tau_p}}. \quad (22)$$

which yields the optimum bias current by using (20):

$$I_{0_{Optimum}} = I_{th} + \frac{qV_p}{V_g a \eta_i \tau_e \tau_p}. \quad (23)$$

By increasing the bias current over the threshold as shown in the above equation, and using the modulation frequency given by (22) one has the optimal operation point.

As a result, the maximum value of the first harmonic power is given by

$$\left(\frac{P_1(j\omega)}{I_1(j\omega)}\right)_{Max} = -j \frac{hv\eta_i}{2\tau_m q \sqrt{\tau_e \tau_p}} \quad (24)$$

3 Results and Discussion

3.1 First and Second Harmonic Powers

As demonstrated in the previous section the trend of the first harmonic power on the peak curve (20) is not monotonic as shown in Fig. 2, and has a maximum which is calculated; after passing this unique maximum, it diminishes slowly.

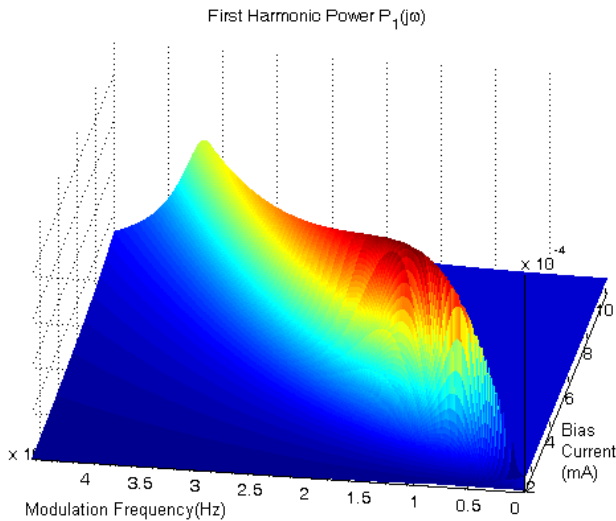


Fig. 2. The first harmonic power $P_1(j\omega)$ vs. frequency and bias current. ($I_{th} = 1.11$ mA)

The second harmonic power decays quickly by increasing the bias current and modulation frequency as shown in Fig. 3.

The contour plots of Fig. 4 and 5 are completely in agreement with our previous claims.

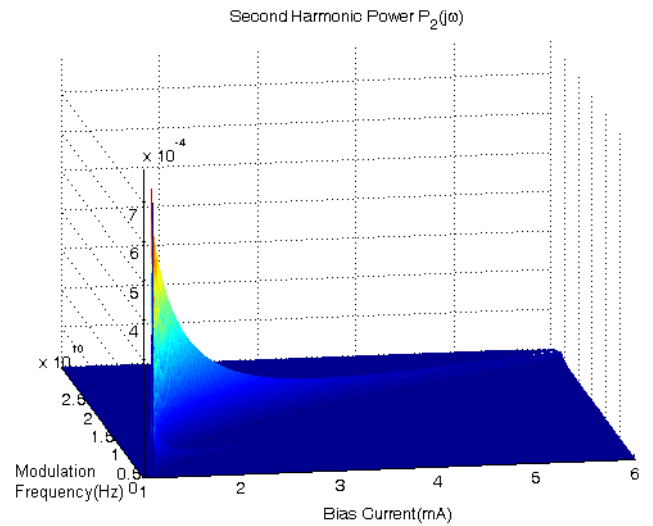


Fig. 3. The second harmonic power $P_2(j\omega)$, vs. frequency and bias current. ($I_{th} = 1.11$ mA)

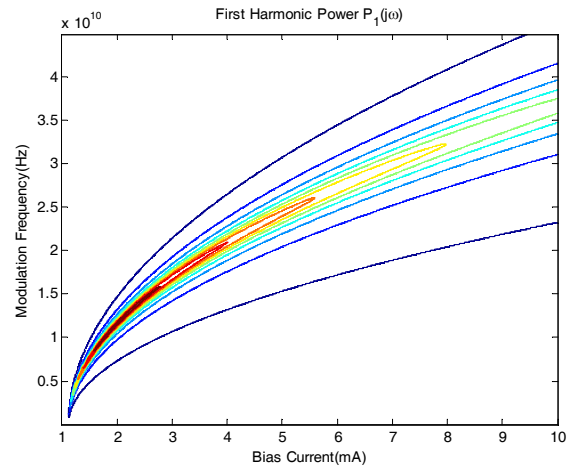


Fig. 4. Contour plot of the first harmonic power $P_1(j\omega)$; vs. frequency and bias current. ($I_{th} = 1.11$ mA)

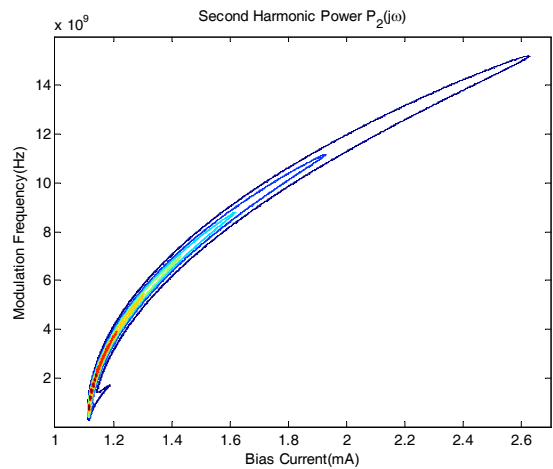


Fig. 5. Contour plot of the second harmonic power $P_2(j\omega)$, vs. frequency and bias current. ($I_{th} = 1.11$ mA)

3.2 Power Distribution between Harmonics

The diagrams of harmonic powers are plotted in Fig. 6 and 7 in a logarithmic scale. The first four resonant frequencies can be seen, and compared.

In bias currents near to the threshold we observe that the power of upper harmonics (second, third, and fourth) exceed the power of the first harmonic in frequencies near the resonant frequencies because of high nonlinearity. This issue is shown in Fig. 6. If we increase the bias current the power content of upper harmonics suppress as shown in the Fig. 7. If the bias current increases further, the power of higher harmonics diminishes very fast; thus, can be neglected.

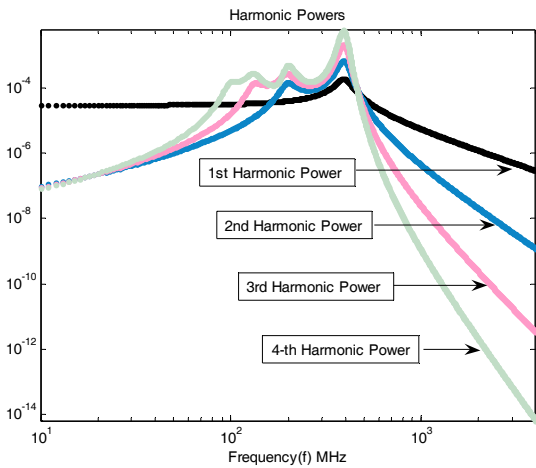


Fig. 6. Harmonic power versus frequency; Bias current: 1.15 mA, ($I_{th} = 1.11$ mA)

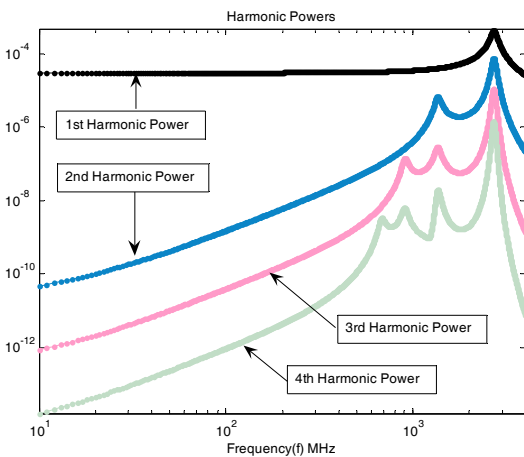


Fig. 7. Harmonic power versus frequency; Bias current: 3mA ($I_{th} = 1.11$ mA)

In order to distinguish the share of each harmonic in the total power applied to the laser diode, the percentages of power distribution in first four harmonics are shown in Fig. 8 and 9. Here we have considered enough harmonics to calculate the total power applied.

The same as Fig. 6 and 7 in the bias currents near the threshold, higher harmonics absorb more power than the first one. Therefore, we expect to observe distortions near threshold. If we increase the bias current further the higher harmonics suppress to negligible percentages. The relating diagrams can be seen in Fig. 8 and 9 respectively.

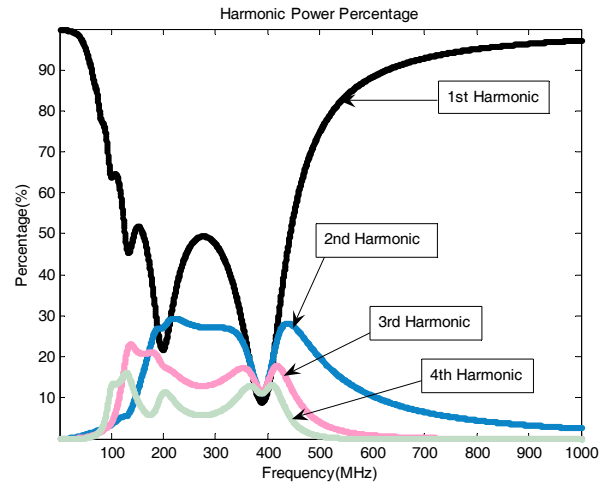


Fig. 8. Harmonic power percentage over all harmonic powers versus frequency (first four harmonics are shown); Bias current: 1.15 mA, ($I_{th} = 1.11$ mA).

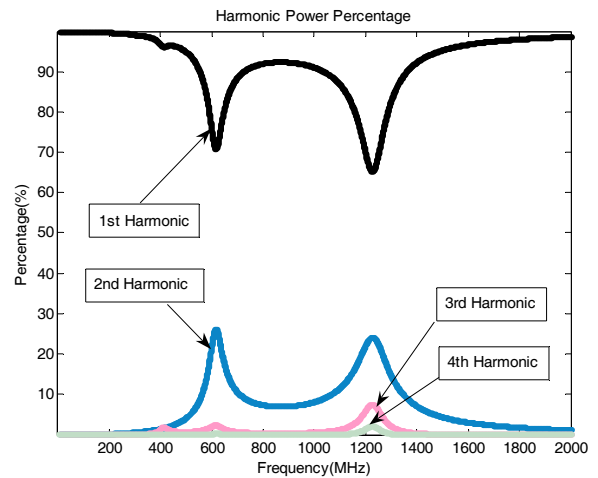


Fig. 9. Harmonic power percentage over all harmonic powers versus frequency (first four harmonics are shown); Bias current: 1.5 mA, ($I_{th} = 1.11$ mA).

The amplitudes of the first and the second harmonics on the peak curve (20) are plotted in Fig. 10. The optimal operation point for the first harmonic power calculated by this approach exactly coincides with the point observed in the mentioned figure. Although we anticipate distortions near threshold the second harmonic power is much higher than its expected value. This issue can also be observed for higher harmonics more severely. This is shown in a semi-logarithmic scale in Fig. 11 It seems that this state cannot be explained by rate equations, and in practice regardless of the

distortions near the threshold current the amplitude of the harmonic powers are confined.

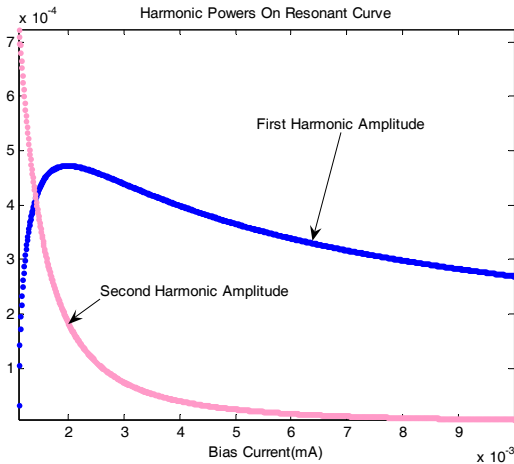


Fig. 10. Harmonic powers on peak curve (first resonant frequency) versus bias current, ($I_{th} = 1.11$ mA).

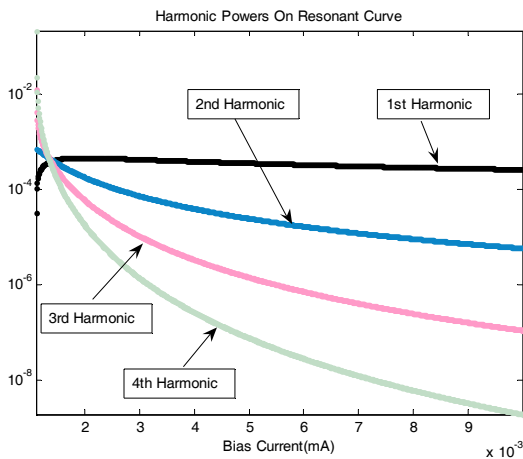


Fig. 11. Harmonic powers on peak curve (first resonant frequency) versus bias current in semi-logarithmic scale. ($I_{th} = 1.11$ mA);

4 Conclusion

We have extracted the recursion expression for the power of each harmonic, and shown that the resonant frequency for the n -th harmonic is proportional to the Relaxation Resonance Frequency for the first harmonic. We have also demonstrated that due to the Lorentzian characteristic of the output power, the maximum of the optical output power for each harmonic occurs at the first harmonic resonant frequency. Moreover, due to the square root dependence of the resonant frequency to the bias current, one can tune the input current to obtain the desired Relaxation Resonance Frequency. The optimal operation point for gaining the highest primary harmonic power is calculated. The results of this study can be helpful in the design, and optimization of nonlinear distortions, which are naturally associated with the transmission of a signal by a semiconductor laser diode.

References:

- [1] L. A. Coldren and S. W. Corzine, *Diode lasers and photonic integrated circuits*, John Wiley & Sons, 1995.
- [2] J. C. Cartledge, and R. C. Srinivasan, Extraction of DFB laser rate equation parameters for system simulation purposes, *J. Lightwave Technol.*, Vol. 15, No. 5, 1997, pp 852-860.
- [3] H. M. Salgado, J. M. Ferreira, and J. J. O'Reilly, Extraction of semiconductor intrinsic laser parameters by intermodulation distortion analysis, *IEEE Photonics Technol. Lett.*, Vol. 9, No. 10, 1997, pp. 1331-1333.
- [4] A. Sharaiha, Harmonic and intermodulation distortion analysis by perturbation and harmonic balance methods for in-line photodetection in a semiconductor optical amplifier, *IEEE Photonics Technol. Lett.*, Vol. 10, No. 3, 1998, pp. 421-423.
- [5] A. Sharaiha, Distortion analysis of the photo-detection and gain spectral responses of a semiconductor optical amplifier, *IEEE Photonics Technol. Lett.*, Vol. 10, No. 9, 1998, pp. 1301-1303.
- [6] P. S. André, A. Nolasco Pinto, J. L. Pinto, and F. da Rocha, Extraction of laser rate equations parameters, *Proc. SPIE*, Vol. 3572, No. 141, 1999.
- [7] J. Chen, R. J. Ram, and R. Helkey, Linearity and third-order intermodulation distortion in DFB semiconductor lasers, *IEEE J. Quantum Electron.*, Vol. 35, No. 8, 1999, pp. 1231-1237.
- [8] G. Morthier, R. Schatz, and O. Kjebon, Extended modulation bandwidth of DBR and external cavity lasers by utilizing a cavity resonance for equalization, *IEEE J. Quantum Electron.*, Vol. 36, No. 12, Dec. 2000, pp. 1468-1475.
- [9] R. Yildirim, and M. Schetzen, Applications of the single-mode laser-diode system theory, *Opt. Commun.*, Vol. 219, Nov. 2002, pp. 351-355.
- [10] S. Ghoniemy, L. MacEachern, and S. Mahmoud, Extended robust semiconductor laser modeling for analog optical link simulations, *IEEE J. of Selected Topics in Quantum Electron.*, Vol. 9, No. 3, Jun. 2003, pp. 872- 878.
- [11] H. Zandi, M. Bavafa, M. Chamanzar, and S. Khorasani, Analysis of power harmonic content and relaxation resonant frequency of a diode laser, *Proc. SPIE*, Vol. 6468, No. 64680J, 2007.
- [12] H. Zandi, M. Bavafa, M. Chamanzar, and S. Khorasani, Harmonic content and relaxation resonant frequency of a modulated laser diode, submitted to *IEEE J. Quantum Electron.*